A New Fractional-Order Adaptive Interval Type-3 Fuzzy Logic-Backstepping Control Algorithm of Doubly Fed Induction Generators

Tarek Aounallah, Nawal Ferhat, Najib Essounbouli, Abdelaziz Hamzaoui

IEEE Access
Multidisciplinary ⋮ Rapid Review ⋮ Open Access Journal

Received 4 May 2025, accepted 22 May 2025, date of publication 30 May 2025, date of current version 6 June 2025.

Digital Object Identifier 10.1109/ACCESS.2025.3575048

RESEARCH ARTICLE

A New Fractional-Order Adaptive Interval Type-3 Fuzzy Logic-Backstepping Control Algorithm of Doubly Fed Induction Generators

TAREK AOUNALLAH[1], NAWAL FERHAT[1,2], NAJIB ESSOUNBOULI[1], AND ABDELAZIZ HAMZAOUI[1]

[1]CReSTIC, University of Reims Champagne-Ardenne, Campus Moulin de la Housse, 51100 Reims, France
[2]LINS, University of Science and Technology Houari Boumediene, Algiers 16111, Algeria

Corresponding authors: Tarek Aounallah (tarek.aounallah@univ-reims.fr) and Nawal Ferhat (nawal.ferhat@univ-reims.fr)

ABSTRACT This paper presents a new fractional-order control algorithm for a doubly fed induction generator-based wind energy conversion system. Nonlinearities resulting from wind turbine dynamics, parametric uncertainties due to generator modeling, and stochastic wind disturbances can seriously affect control performances and consequently decrease wind power extraction. The suggested approach combines interval type 3 adaptive fuzzy systems with a backstepping control technique to improve the quality of the closed-loop response and the robustness of the system. Besides approximating nonlinear functions, interval type 3 fuzzy systems are used to handle a higher level of uncertainty compared to type 1 or type 2 fuzzy logic approaches. The stability analysis is proved according to the Lyapunov method extended to fractional order. Several simulation results are presented accompanied by a comparative study with some other well-known fuzzy backstepping methods.

INDEX TERMS Interval type 3 fuzzy logic system, general type 2 fuzzy logic system, interval type 2 fuzzy logic system, backstepping, fractional-order, DFIG, Lyapunov.

I. INTRODUCTION

In response to climate change and inclusive transition towards carbon neutrality, social and industrial demands for renewable energy have significantly increased in recent decades. This has led to continued advancements in wind turbine technology, known as one of the most efficient, cost-effective, and environmentally friendly of electrical energy sources [1].

Central to this technology is the electric generator, which embedded within the wind turbine, performs the critical function to convert turbine's mechanical energy into electrical power. The Doubly Fed Induction Generator (DFIG) has a long tradition in wind power stations due to their robustness, cost-effectiveness, and ability to generate reactive power to support the grid [1], [2].

The associate editor coordinating the review of this manuscript and approving it for publication was Norbert Herencsar.

However, the design of control algorithms for the DFIG based wind turbines is concorded as a challenging task. The control performance can be impacted by various factors such as nonlinear phenomena from dynamic behavior of wind turbines, electrical faults, thermal issues, uncertainties in generator modeling, and external environmental factors. These factors can change the expected system behavior and drastically decrease the extraction of wind energy.

Several studies have been proposed in the literature for an effective control of the DFIG connected to the grid. Among these studies, we can cite the conventional control methods which, in their cascaded control loops, involve simple Proportional-Integral (PI) controllers [3], PI-neural network [4], or PI-neural fuzzy systems [5]. A major drawback of this category of controllers is that they are designed using a linear approach which involves some approximations and simplifying assumptions. This results in a limited control performance due to the highly nonlinear characteristics of the wind turbine.

In this regard, various advanced methods address this problem, such as sliding mode control and its various improvements [6], [7], fuzzy logic control techniques [8], [9], [10], [11], [12], the backstepping approach [13], [14], [15], [16], etc.

Backstepping control approach is a systematic design technique that breaks down a complex nonlinear system into simpler recursive subsets. However, a perfect machine parameters knowledge is crucial in conventional backstepping control design. To overcome this weakness, fuzzy systems have been proposed to approximate the model nonlinear functions and manage uncertainties and/or imprecisions [17], [18]. Based on Lyapunov's stability theory, the resulting control laws aim to ensure stabilization, regulation, and control of nonlinear dynamic systems. Furthermore, the backstepping design method can easily be combined with adaptive fuzzy control techniques [19], [20], [21], [22].

To improve the approximation capability of the fuzzy systems, some aspects of the General Type 2 Fuzzy Logic System (GT2-FLS) have been studied. Unlike the Interval Type 2 Fuzzy Logic System (IT2-FLS), where the secondary membership is a fixed number, in GT2-FLS, it is obtained from a Type 1 fuzzy set. This results in better performance and more ability to cope with uncertainties compared to IT2-FLS [17], [18]. In order to handle more level of uncertainties, the IT3-FLS has been introduced, where the secondary membership set is an interval Type 2 fuzzy one. Various engineering applications demonstrate the effectiveness of IT3-FLS [23], [24], [25]. However, it remains rarely studied in generator control.

Otherwise, several traditional control methods have been extended to fractional-order operators to enhance the control performance from different aspects [26], [27], [28]. Furthermore, fractional order calculus remains the more suitable technique to model DFIG since its inductance has a fractional order characteristic, and the electrical state variables have different orders from those of the rotor motion state variables [29].

In this article, a new fractional order adaptive robust control method is designed for a DFIG based variable speed wind turbine. Applied to the converter side generator, the objective of this strategy is to improve robustness performance and closed-loop response.

The contributions of this paper are summarized as follows:

1) A fractional order adaptive interval Type 3 fuzzy backstepping control is presented and compared with the other backstepping approaches using GT2, IT2 and T1 adaptive fuzzy systems.
2) Fractional calculus is used in DFIG modeling, fuzzy systems and backstepping control scheme.
3) The adaptation laws are obtained on-line from the stability analysis of the extended fractional Lyapunov theorem.

Combining backstepping control and new generation of fuzzy systems in this works, is motivated by: (i) backstepping control is the more suitable to obtain good performance for DFIG control [30]. (ii) according to [31], moving from IT2-FLS to IT3-FLs allows to increase the capability of the fuzzy system to manage uncertainties and hence to improve the modeling precision.

Simulation results demonstrate the superiority of the proposed control approach compared to some other fuzzy backstepping methods. The paper is organized as follows. In Section II, fractional order concepts and system modeling are described. The control algorithm and stability analysis are illustrated in Section III. The simulations and results are provided in Section IV, and finally the conclusion in Section V. The main abbreviations used in this paper are summarized in Table 1.

TABLE 1. Abbreviations and their definitions.

Abbreviations	Definitions
DFIG	Doubly Fed Induction Generator
PI	Proportional Integral
MF	Membership function
T1-FLS	Type 1 Fuzzy Logic System
IT2-FLS	Interval Type 2 Fuzzy Logic System
GT2-FLS	General Type 2 Fuzzy Logic System
IT3-FLS	Interval Type 3 Fuzzy Logic System
FT1-FLS	Fractional Type 1 Fuzzy Logic System
FIT2-FLS	Fractional Interval Type 2 Fuzzy Logic System
FGT2-FLS	Fractional General Type 2 Fuzzy Logic System
FIT3-FLS	Fractional Interval Type 3 Fuzzy Logic System
ITAE	Integral Time Absolute Error
ISE	Integral Square Error

II. MATHEMATICAL PRELIMINARIES AND DFIG MODELING

A. FRACTIONAL DEFINITIONS

This section briefly describes the definitions concerning the fractional order calculus used in this paper [32]. Considering the following fractional order differential-integral operator ${}_{t_0}D_t^m$:

$$ {}_{t0}D_t^m = \begin{cases} \dfrac{d^m}{dt^m} & \Re(m) > 0 \\ 1 & \Re(m) = 0 \\ \displaystyle\int_{t_0}^{t} (dt)^{-m} & \Re(m) < 0 \end{cases} \tag{1} $$

where:

$m \in \mathbb{C}$ is a complex number that denotes the fractional order and $\Re(m)$ is the real part of m. The mathematical expressions of the Riemann-Liouville derivative and integral are given as follows:

- Expression of the derivative

$$ {}_{t_0}^{RL}D_t^m f(t) = \frac{1}{\Gamma(n-m)} \frac{d^n}{dt^n} \int_{t_0}^{t} (t-\tau)^{n-m-1} f(\tau) d\tau \tag{2} $$

- Expression of the integral

$$ {}_{t_0}^{RL}I_t^m f(t) = \frac{1}{\Gamma(m)} \int_{t_0}^{t} (t-\tau)^{m-1} f(\tau) d\tau \tag{3}$$

where:

$\Gamma(x) = \int_0^{\infty} y^{x-1} e^{-y} dy$

$x < 0$ and $(n-1) < m < n, n \in \mathbb{Z}$

B. SYSTEM DESCRIPTION

Fig. 1 shows the selected configuration of the DFIG control system, which includes the aerodynamic subsystem, drive-train part, and back-to-back converter. The rotor windings are connected to the back-to-back converter via slip rings, while the stator is directly connected to the grid through an electrical transformer. In this paper, the control scheme is mainly focused on the generator side converter. The power electronic interface allows, through control loops of torque/rotational-speed and rotor currents (in d-q framework with stator flux orientation), to obtain a maximum extracted energy for various wind speeds.

The mathematical expressions of the DFIG power equations are given as follows:

$$\begin{cases} V_{ds} = R_s I_{ds} + D^m \varphi_{ds} - \omega_s \varphi_{qs} \\ V_{dr} = R_r I_{dr} + D^m \varphi_{dr} - \omega_r \varphi_{qr} \\ V_{qs} = R_s I_{q(s,r)} + D^m \varphi_{qs} + \omega_s \varphi_{ds} \\ V_{qr} = R_r I_{q(s,r)} + D^m \varphi_{qr} + \omega_r \varphi_{dr} \\ \varphi_{ds} = L_s I_{ds} + L_m I_{dr} \\ \varphi_{dr} = L_r I_{dr} + L_m I_{ds} \\ \varphi_{qs} = L_s I_{qs} + L_m I_{qr} \\ \varphi_{qr} = L_r I_{qr} + L_m I_{qs} \end{cases} \tag{4}$$

where:

V_{ds}, V_{dr}, V_{qs}, *and* V_{qr}: are the stator/rotor voltages in d-q framework

I_{ds}, I_{dr}, I_{qs}, *and* I_{qr}: are the stator/rotor currents in d-q framework

R_s, R_r: are the stator/rotor resistance

L_s, L_r, *and* L_m: are the stator/rotor and mutual inductances

$\varphi_{ds}, \varphi_{dr}, \varphi_{qs}$, *and* φ_{qr}: are the stator/rotor fluxes

ω_s, ω_r: are the stator/rotor electric pulsations

The expressions of mechanical equations are given as:

$$J D^m \Omega + f\Omega = \Gamma_g - P\frac{3}{2}\frac{L_m}{L_s}(I_{dr}\varphi_{qs} - I_{qr}\varphi_{ds}) \tag{5}$$

where:

Γ_g: is the generator torque

J: is the generator inertia

f: is the viscous friction coefficient

Ω: is the angular mechanic velocity

P: is the number of pairs poles

$\Omega = D^m\theta$, $\omega = D^m\theta_e$ and $\theta_e = P\ \theta$

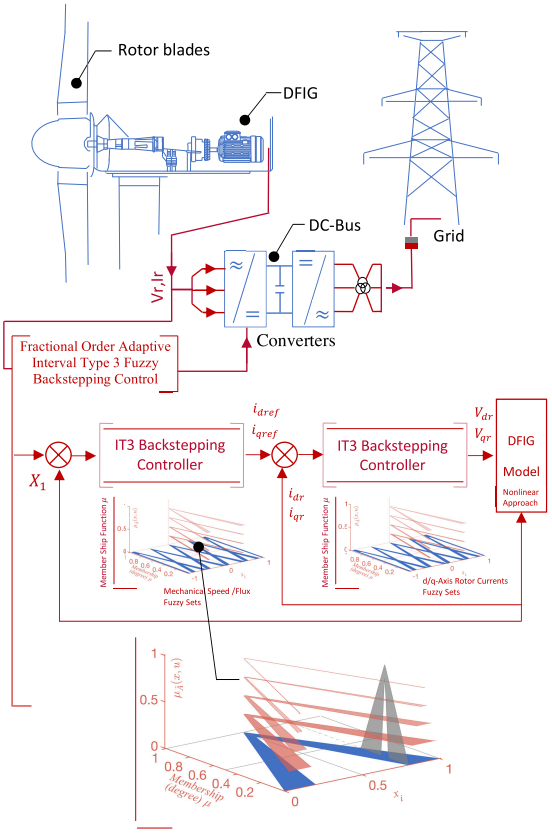

FIGURE 1. DFIG based wind energy's conversion system.

The mathematical expressions for the generated active (P_s) and reactive (Q_s) powers are given as follows:

$$\begin{cases} P_s = \frac{3}{2}(V_{ds}I_{ds} + V_{qs}I_{qs}) \\ Q_s = \frac{3}{2}(V_{qs}I_{ds} - V_{ds}I_{qs}) \end{cases} \tag{6}$$

Based on the direct field-oriented control and after some mathematical manipulations, the DFIG dynamic representation can be rewritten as follows:

$$\begin{cases} D^m I_{dr} = -\kappa I_{dr} + \omega_r I_{qr} + \alpha_s \frac{L_m}{L_s \sigma_r}\varphi_{ds} + \varrho_1 \\ D^m I_{qr} = -\kappa I_{qr} - \omega_r I_{dr} + \frac{L_m}{L_s \sigma_r}\omega\varphi_{ds} + \varrho_2 \\ D^m \varphi_{ds} = \frac{R_s}{L_s}(-\varphi_{ds} + L_m I_{dr}) + V_{ds} \\ D^m \omega = \frac{1}{J}(-P^2\frac{3}{2}\frac{L_m}{L_s}\left(I_{dr}\varphi_{qs} - I_{qr}\varphi_{ds}\right) + \left(P\Gamma_g - f\omega\right)) \end{cases} \tag{7}$$

with:

$$\omega_r = \omega_s - \omega$$

$$\kappa = \frac{R_r}{\sigma_r} + \frac{R_s L_m^2}{L_s^2 \sigma_r}$$

$$\varrho_1 = -\frac{L_m}{L_s \sigma_r} V_{ds} + \left(\frac{1}{\sigma_r}\right) V_{dr}$$

$$\varrho_2 = -\frac{L_m}{L_s\sigma_r}V_{qs} + \left(\frac{1}{\sigma_r}\right)V_{qr}$$

The fractional order model of the generator can be written in a compact form as follows:

$$\begin{cases} D^m X_1 = F_1 + X_2 + \Delta_1 \\ D^m X_2 = F_2 + U + \Delta_2 \end{cases} \tag{8}$$

where:
$X_1 = [\omega \quad \varphi_{ds}]^T$: denotes the system inputs
$U = \begin{bmatrix} V_{qr} & V_{dr} \end{bmatrix}^T$: denotes the system outputs
$X_2 = \begin{bmatrix} I_{qr} & I_{dr} \end{bmatrix}^T$: denotes the intermediate inputs
Δ_1 and Δ_2: represent disturbances

Expressions of elements of the above mathematical equations are given by:

$$\begin{cases} F_1 = \left(1 - b_1^{-1}\right) D^m X_1 + b_1^{-1} f_1 \\ \Delta_1 = [\Delta_{11} \quad \Delta_{12}]^T \\ \quad = b_1^{-1}\delta_1 \\ F_2 = \left(1 - b_2^{-1}\right) D^m X_2 + b_2^{-1} f_2 \\ \Delta_2 = [\Delta_{21} \quad \Delta_{22}]^T \\ \quad = b_2^{-1}\delta_2 \end{cases} \tag{9}$$

with:

$$f_1 = \begin{bmatrix} -\frac{f}{J}\omega & -\frac{R_s}{L_s}\varphi_{ds} \end{bmatrix}^T$$

$$f_2 = [\beta_1 \quad \beta_2]^T$$

$$\beta_1 = \left[I_{dr}\ell_1 + I_{qr}(\omega_s - \omega) + \varphi_{ds}\left(\frac{-R_s L_s \ell_1}{{L_s}^2 + R_s}\right)\right]$$

$$\beta_2 = \left[I_{qr}\ell_1 - I_{dr}(\omega_s - \omega) + \omega\varphi_{ds}\left(\frac{-\ell_1}{L_s^2 + R_s}\right)\right]$$

$$\ell_1 = \frac{-L_s^2 - R_s}{L_r L_s^2\left(1 - \frac{L_m^2}{L_r L_s}\right)}$$

$$b_1 = [\beta_3 \quad \beta_4]^T, b_2 = [\beta_5 \quad \beta_6]^T$$

$$\beta_3 = \left[0 \quad \varphi_{ds}\frac{P^2 L_m}{J L_s}\right], \beta_4 = \left[\frac{R_s L_m}{L_S} \quad 0\right]$$

$$\beta_5 = \left[\frac{L_s^2\ell_1}{L_s^2 + R_s} \quad 0\right], \beta_6 = \left[0 \quad \frac{L_s^2\ell_1}{L_s^2 + R_s}\right]$$

$$\delta_1 = \left[\frac{P}{J}\Gamma_g \quad V_{ds}\right]^T$$

$$\delta_2 = \left[\frac{-V_{ds}L_m L_s \ell_1}{L_s^2 + R_s} \quad \frac{-V_{qs}L_m L_s \ell_1}{L_s^2 + R_s}\right]^T$$

III. FRACTIONAL-ORDER ADAPTIVE FUZZY BACKSTEPPING CONTROLLER

In this section, the synthesis of fractional adaptive fuzzy Backstepping control methods is detailed step-by-step. The idea is to design an appropriate control input U allowing to achieve the tracking objectives (i.e.: the alignment of X_1 on its reference signal $Y_{ref} = \begin{bmatrix} \omega_{ref} & \varphi_{s\,ref} \end{bmatrix}^T$).

■ First, we define the tracking error as:

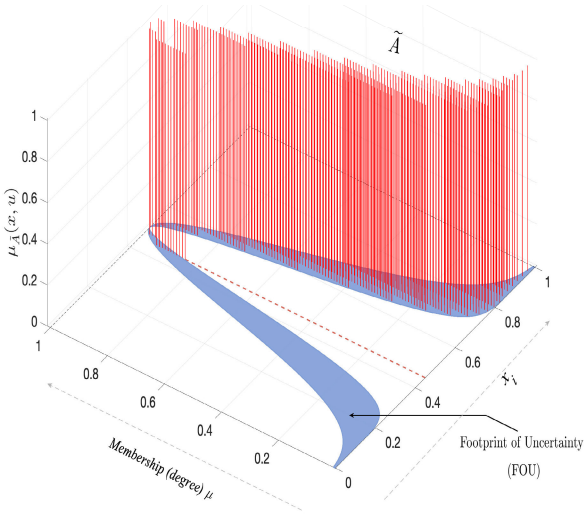

FIGURE 2. The interval type 2 gaussian membership function.

$$e_1 = Y_{ref} - X_1 \tag{10}$$

Its fractional time derivative is given by:

$$D^m e_1 = D^m Y_{ref} - F_1 - X_2 - \Delta_1 \tag{11}$$

Using the following Lyapunov function:

$$V_1 = \frac{1}{2}e_1^T e_1 \tag{12}$$

We therefore have [33]:

$$\begin{cases} D^m V_1 \leq e_1^T D^m e_1 \\ \qquad \leq e_1^T (D^m Y_{ref} - F_1 - X_2 - \Delta_1) \end{cases} \tag{13}$$

■ To satisfy the stability requirement $D^m V_1 < 0$, we define a second error e_2 between X_2 and its desired value X_{2d} (namely intermediate or virtual control law) as follows:

$$\begin{cases} e_2 = X_{2d} - X_2 \\ X_{2d} = X_{2d_{eq}} + c_1 e_1 + k_1 sign(e_1) \end{cases} \tag{14}$$

where $X_{2d_{eq}} = D^m Y_{ref} - F_1$ and c_1 is a positive constant.

Based on the fact that the function F_1 is considered unknown, the next step is to estimate $X_{2d_{eq}}$ by a fuzzy system.

A. FRACTIONAL ADAPTIVE IT2-FLS BACKSTEPPING METHOD

As shown in Fig. 2, the secondary membership function (MF) in the IT2MF is constant [17], [18].

The output of the IT-2 fuzzy system can be written as:

$$f_{\left(\zeta_{(1)L,R}^T,\ \theta_{(1)L,R}\right)} = \frac{1}{2}\left(\zeta_{(1)L}^T\theta_{(1)L} + \zeta_{(1)R}^T\theta_{(1)R}\right) \tag{15}$$

with:

$\zeta_{(1)_L}, \zeta_{(1)_R}$: left and right adjustable parameter vectors
$\theta_{(1)_L}, \theta_{(1)_R}$: regressive vectors
$\theta^*_{(1)_{L,R}} = \theta_{(1)_{L,R}} - \tilde{\theta}_{(1)_{L,R}}$
$\theta^*_{(\cdot)_L}, \theta^*_{(\cdot)_R}$: optimal parameter vectors
$\tilde{\theta}_{(1)_L}, \tilde{\theta}_{(1)_R}$: estimation errors

The tracking error equation 11 can be rewritten as:

$$D^m e_1 = -c_1 e_1 - f_{e1} + e_2 - f_{\left(\zeta^T_{(1)_{L,R}}, \tilde{\theta}_{(1)_{L,R}}\right)} + w_1 \quad (16)$$

where:
$f_{e1} = k_1 sign(e_1) + \Delta_1$
$w_1 = X^*_{2d} - X_{2d}$: is the minimal approximation error.
At this step, the control stability is guaranteed with the following new Lyapunov function:

$$V_1 = \frac{1}{2} e_1^T e_1 + \frac{1}{2}\left(\frac{1}{\gamma_{(1)_L}} \tilde{\theta}^T_{(1)_L} \tilde{\theta}_{(1)_L} + \frac{1}{\gamma_{(1)_R}} \tilde{\theta}^T_{(1)_R} \tilde{\theta}_{(1)_R}\right) \quad (17)$$

where $\gamma_{(1)_L}$ and $\gamma_{(1)_R}$ are the learning rates.
Using equation 16, the fractional time derivative is:

$$D^m V_1 = e_1^T \psi + h_{\left(\gamma_{(1)_{L,R}}\ ,\ \tilde{\theta}_{(1)_{L,R}}\right)} \quad (18)$$

where:

$$\psi = (-c_1 e_1 - f_{e1} + e_2 + w_1 - f_{\left(\zeta^T_{(1)_{L,R}}\ ,\ \tilde{\theta}_{(1)_{L,R}}\right)})$$

$$h_{\left(\gamma_{(1)_{L,R}}\ ,\ \tilde{\theta}_{(1)_{L,R}}\right)} = \frac{1}{\gamma_{1L}} \tilde{\theta}^T_{1L} D^m \tilde{\theta}_{1L} + \frac{1}{\gamma_{1R}} \tilde{\theta}^T_{1R} D^m \tilde{\theta}_{1R}$$

According to the previous assumptions, the second tracking error is given by:

$$D^m e_2 = D^m X_{2d} - (F_2 + U + \Delta_2) \quad (19)$$

The stability function that includes the two control errors is:

$$V_2 = \frac{1}{2} e_1^T e_1 + \frac{1}{2} e_2^T e_2 \quad (20)$$

The control law expression that allows to have $D^m V_2 < 0$ can be considered as follows:

$$U = D^m X_{2d} - F_2 + e_1 + c_2 e_2 + k_2 sign(e_2) \quad (21)$$

where: $U_{eq} = D^m X_{2d} - F_2$
Using the same approach to approximate U_{eq}, the second error equation can be rewritten as:

$$D^m e_2 = -c_2 e_2 - f_{e2} - e_1 - w_2 - f_{\left(\zeta^T_{(2)L,R}, \tilde{\theta}_{(2)L,R}\right)} \quad (22)$$

where:
$f_{e2} = k_2 sign(e_2) + \Delta_2$
$w_2 = U^*_{eq} - U_{eq}$: is the minimal approximation of the second error.
The global convergence function is given as below:

$$V_2 = V_1 + \frac{1}{2} e_2^T e_2 + \frac{1}{2}\left(\frac{1}{\gamma_{2L}} \tilde{\theta}^T_{2L} \tilde{\theta}_{2L} + \frac{1}{\gamma_{2R}} \tilde{\theta}^T_{2R} \tilde{\theta}_{2R}\right) \quad (23)$$

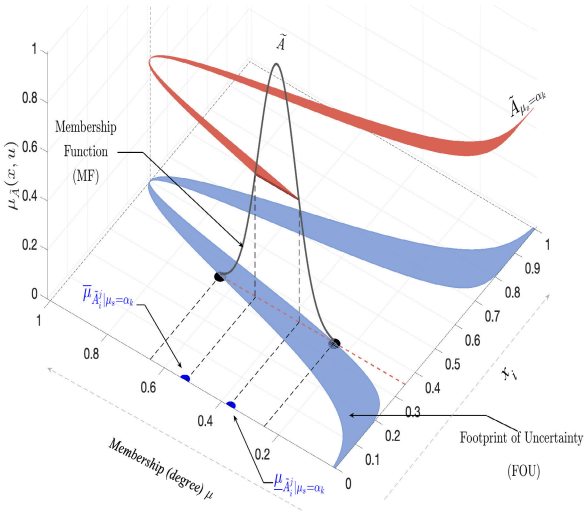

FIGURE 3. The general type 2 gaussian membership function.

Its fractional time derivative is:

$$D^m V_2 = D^m V_1 + e_2^T D^m e_2 + h_{\left(\gamma_{(2)_{L,R}}\ ,\ \tilde{\theta}_{(2)_{L,R}}\right)} \quad (24)$$

where $h_{\left(\gamma_{(2)_{L,R}}, \tilde{\theta}_{(2)_{L,R}}\right)} = \frac{1}{\gamma_{2L}} \tilde{\theta}^T_{2L} D^m \tilde{\theta}_{2L} + \frac{1}{\gamma_{2R}} \tilde{\theta}^T_{2R} D^m \tilde{\theta}_{2R}$.
Using the following adaptation law:

$$D^m \theta_{(2)_{L,R}} = \frac{1}{2} \gamma_{(2)_{L,R}} \zeta_{(2)_{L,R}} e_2 \quad (25)$$

Equation 24 becomes:

$$D^m V_2 < -c_1 e_1^T e_1 - c_2 e_2^T e_2 \quad (26)$$

This result proves that the proposed approach guarantees stability in the Lyapunov sense.

Remark 1: Δ_1 and Δ_2 are bounded by two positive scalars k_1 and k_2 ($\|\Delta_1\| < k_1, \|\Delta_2\| < k_2$), c_1 and c_2 are strictly positive constants such that the stability of the closed loop system is guaranteed.

B. FRACTIONAL ADAPTIVE GT2-FLS BACKSTEPPING METHOD

As illustrated in Fig.3, the secondary MF of the General Type 2 fuzzy logic is a Type 1 MF [17], [18].
The mathematical expression of the output GT2 FLS is:

$$f_{\left(\zeta^T_{(\alpha)_{L,R}}, \theta_{(\alpha)_{L,R}}\right)} = \sum_{k=1}^{N} \left(K_{\alpha_k}\left[\frac{\theta^T_{l\alpha_k} \xi_{l\alpha_k} + \theta^T_{r\alpha_k} \xi_{r\alpha_k}}{2}\right]\right) \quad (27)$$

with:
$\zeta_{(\alpha)_L}, \zeta_{(\alpha)_R}$: designate the left and right adjustable parameter vectors
$\theta_{(\alpha)_L}, \theta_{(\alpha)_R}$: are the regressive vectors
$\theta^*_{(\alpha)_{L,R}} = \theta_{(\alpha)_{L,R}} - \tilde{\theta}_{(\alpha)_{L,R}}$
$\theta^*_{(\alpha)_L}, \theta^*_{(\alpha)_R}$: are the optimal parameter vectors
$\tilde{\theta}_{(\alpha)_L}, \tilde{\theta}_{(\alpha)_R}$: are the estimation errors

Its tracking error is:

$$D^m e_1 = -c_1 e_1 - f_{e1} + e_2 - f_{\left(\zeta^T_{1(\alpha)_{L,R}}, \tilde{\theta}_{1(\alpha)_{L,R}}\right)} + w_1 \quad (28)$$

where:
$f_{e1} = k_1 sign\,(e_1) + \Delta_1$
$w_1 = X^*_{2d} - X_{2d}$: is minimal approximation error
The new Lyapunov function V_1 is given as:

$$\begin{aligned} V_1 = &\frac{1}{2} e_1^T e_1 \\ &\times \sum_{k=1}^{N} \frac{1}{2\gamma_{1L\alpha_k x}} \tilde{\theta}^T_{1L\alpha_k} \tilde{\theta}_{1L\alpha_k} \\ &\times \sum_{k=1}^{N} \frac{1}{2\gamma_{1R\alpha_k x}} \tilde{\theta}^T_{1R\alpha_k} \tilde{\theta}_{1R\alpha_k} \end{aligned} \quad (29)$$

where: $\gamma_{1L\alpha_k x}, \gamma_{1R\alpha_k x}, \gamma_{1L\alpha_k x}, \gamma_{1R\alpha_k x}$ are the learning rates.
It's time derivate is:

$$D^m V_1 \le e_1^T \psi + h_{\left(\gamma_{1(\alpha)_{L,R}}\ ,\ \tilde{\theta}_{1(\alpha)_{L,R}}\right)} \quad (30)$$

with:

$$\begin{aligned} \psi = &-c_1 e_1 - f_{e1} + e_2 + w_1 \\ &- f_{\left(\zeta^T_{1(\alpha)_{L,R}}, \tilde{\theta}_{1(\alpha)_{L,R}}\right)} \\ h_{\left(\gamma_{1(\alpha)_{L,R}}, \tilde{\theta}_{1(\alpha)_{L,R}}\right)} = &\sum_{k=1}^{N} \frac{1}{\gamma_{1L\alpha_k x}} \tilde{\theta}^T_{1L\alpha_k} {}^{C}_{t_0}D^m_t \tilde{\theta}_{1L\alpha_k} \\ &+ \sum_{k=1}^{N} \frac{1}{\gamma_{1R\alpha_k x}} \tilde{\theta}^T_{1R\alpha_k} {}^{C}_{t_0}D^m_t \tilde{\theta}_{1R\alpha_k} \end{aligned}$$

As presented previously, the new global convergence function is:

$$\begin{aligned} V_2 = &V_1 + \frac{1}{2} e_2^T e_2 \\ &+ \sum_{k=1}^{N} \frac{1}{2\gamma_{2L\alpha_k x}} \tilde{\theta}^T_{2L\alpha_k} \tilde{\theta}_{2L\alpha_k} \\ &+ \sum_{k=1}^{N} \frac{1}{2\gamma_{2R\alpha_k x}} \tilde{\theta}^T_{2R\alpha_k} \tilde{\theta}_{2R\alpha_k} \end{aligned} \quad (31)$$

Its time derivative is:

$$D^m V_2 \le D^m V_1 + e_2^T D^m e_2 + h_{\left(\gamma_{(2)_{L,R}}\ ,\ \tilde{\theta}_{(2)_{L,R}}\right)} \quad (32)$$

with:

$$\begin{aligned} h_{\left(\gamma_{2(\alpha)_{L,R}}, \tilde{\theta}_{2(\alpha)_{L,R}}\right)} = &\sum_{k=1}^{N} \frac{1}{\gamma_{2L\alpha_k x}} \tilde{\theta}^T_{2L\alpha_k} {}^{C}_{t_0}D^m_t \tilde{\theta}_{2L\alpha_k} \\ &+ \sum_{k=1}^{N} \frac{1}{\gamma_{2R\alpha_k x}} \tilde{\theta}^T_{2R\alpha_k} {}^{C}_{t_0}D^m_t \tilde{\theta}_{2R\alpha_k} \end{aligned}$$

Considering the following adaptation laws:

$$\begin{cases} {}^{C}_{t_0}D^m_t \tilde{\theta}_{1L\alpha_k} = \frac{1}{2}\gamma_{1L\alpha_k x} e(x,t) K_{\alpha_k} \xi_{L\alpha_k}(s) \\ {}^{C}_{t_0}D^m_t \tilde{\theta}_{1R\alpha_k} = \frac{1}{2}\gamma_{1R\alpha_k x} e(x,t) K_{\alpha_k} \xi_{R\alpha_k}(s) \\ {}^{C}_{t_0}D^m_t \tilde{\theta}_{2L\alpha_k} = \frac{1}{2}\gamma_{2L\alpha_k x} e(x,t) K_{\alpha_k} \xi_{L\alpha_k}(s) \\ {}^{C}_{t_0}D^m_t \tilde{\theta}_{2R\alpha_k} = \frac{1}{2}\gamma_{2R\alpha_k x} e(x,t) K_{\alpha_k} \xi_{R\alpha_k}(s) \end{cases} \quad (33)$$

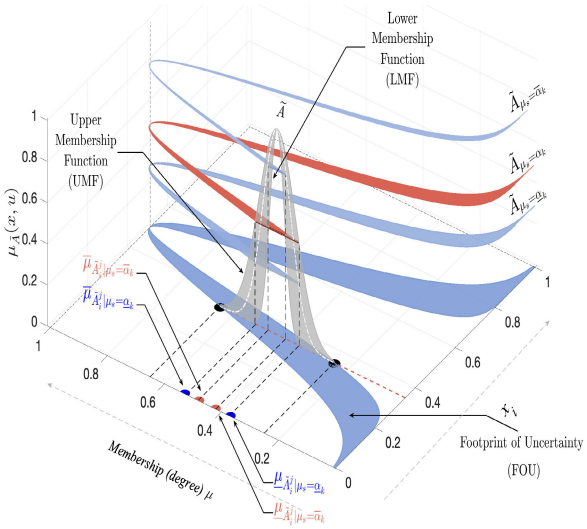

FIGURE 4. The interval type 3 gaussian membership function.

Therefore:

$$D^m V_2 < -c_1 e_1^T e_1 - c_2 e_2^T e_2 \quad (34)$$

with c_1 and c_2 are strictly positive constants.

Finally, we can conclude that the proposed control approach guarantees the global stability.

C. FRACTIONAL ADAPTIVE IT3-FLS BACKSTEPPING METHOD

As shown in Fig.4, the secondary MF of the interval Type 3 is an IT2 MF. The concept of the IT3-FLS is shown in Fig.5, its output is obtained as follows:

1) The inputs of IT3-FLS are: $x_1 \ldots\ldots x_n$
2) Consider five membership functions (MFs) for each input $\tilde{A}^i_j, j = 1, \ldots, M$
3) Get rule firing degrees $\bar{f}_{\bar{\alpha}}, \bar{f}_{\underline{\alpha}}, f_{\underline{\bar{\alpha}}}$ and $f_{\underline{\alpha}}$
4) Compute the output of the proposed fuzzy system

The $X_{2d,eq}$ should be approximated by an IT3 FLS approach:

$$\begin{aligned} f_{\left(\zeta^T_{(\alpha)_{L,R}}\ ,\ \theta_{(\alpha)_{L,R}}\right)} = &\sum_{k=1}^{N} \left(K_{\underline{\alpha}_k} \left[\frac{\theta^T_{l\underline{\alpha}_k} \xi_{l\underline{\alpha}_k} + \theta^T_{r\underline{\alpha}_k} \xi_{r\underline{\alpha}_k}}{2} \right] \right. \\ &\left. + K_{\bar{\alpha}_k} \left[\frac{\theta^T_{l\bar{\alpha}_k} \xi_{l\bar{\alpha}_k} + \theta^T_{r\bar{\alpha}_k} \xi_{r\bar{\alpha}_k}}{2} \right] \right) \end{aligned} \quad (35)$$

where:
$\zeta_{(\alpha)_L}, \zeta_{(\alpha)_R}$: designate the left and right adjustable parameter vectors
$\theta_{(\alpha)_L}, \theta_{(\alpha)_R}$: designate the regressive vectors
$\theta^*_{(\alpha)_{L,R}} = \theta_{(\alpha)_{L,R}} - \tilde{\theta}_{(\alpha)_{L,R}}$
$\tilde{\theta}_{(\alpha)_L}, \tilde{\theta}_{(\alpha)_R}$: are the estimation error
In the next step, the control stability is guaranteed by:

$$V_1 = \frac{1}{2} e_1^T e_1$$

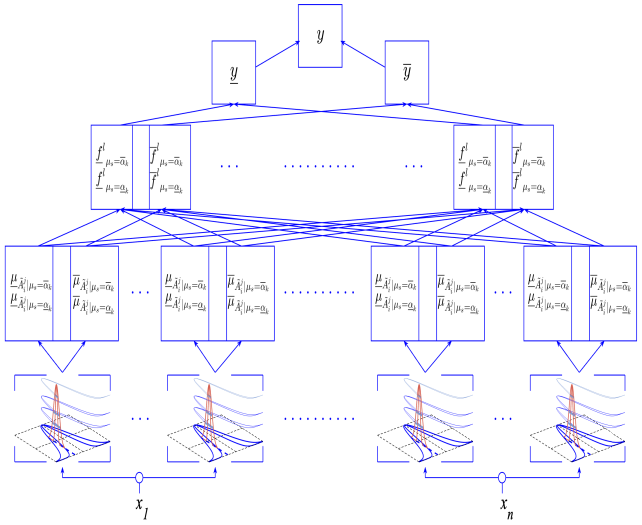

FIGURE 5. IT3 FLS approach.

$$+\sum_{k=1}^{N}\frac{1}{2\gamma_{1L\underline{\alpha}_{k}x}}\tilde{\underline{\theta}}_{1L\underline{\alpha}_{k}}^{T}\tilde{\underline{\theta}}_{1L\underline{\alpha}_{k}}+\sum_{k=1}^{N}\frac{1}{2\gamma_{1R\underline{\alpha}_{k}x}}\tilde{\underline{\theta}}_{1R\underline{\alpha}_{k}}^{T}\tilde{\underline{\theta}}_{1R\underline{\alpha}_{k}}+\sum_{k=1}^{N}\frac{1}{2\gamma_{1L\bar{\alpha}_{k}x}}\tilde{\underline{\theta}}_{1L\bar{\alpha}_{k}}^{T}\tilde{\underline{\theta}}_{1L\bar{\alpha}_{k}}+\sum_{k=1}^{N}\frac{1}{2\gamma_{1R\bar{\alpha}_{k}x}}\tilde{\underline{\theta}}_{1R\bar{\alpha}_{k}}^{T}\tilde{\underline{\theta}}_{1R\bar{\alpha}_{k}} \quad (36)$$

where:

$\tilde{\underline{\theta}}_{1L\underline{\alpha}_{k}}=\underline{\theta}^{*}_{1L\underline{\alpha}_{k}}-\underline{\theta}_{1L\underline{\alpha}_{k}}$; $\tilde{\underline{\theta}}_{1L\bar{\alpha}_{k}}=\underline{\theta}^{*}_{1L\bar{\alpha}_{k}}-\underline{\theta}_{1L\bar{\alpha}_{k}}$

$\tilde{\underline{\theta}}_{1R\underline{\alpha}_{k}}=\underline{\theta}^{*}_{1R\underline{\alpha}_{k}}-\underline{\theta}_{1R\underline{\alpha}_{k}}$; $\tilde{\underline{\theta}}_{1R\bar{\alpha}_{k}}=\underline{\theta}^{*}_{1R\bar{\alpha}_{k}}-\underline{\theta}_{1R\bar{\alpha}_{k}}$

with:

$\underline{\theta}^{*}_{1L\underline{\alpha}_{k}}, \underline{\theta}^{*}_{1R\underline{\alpha}_{k}}, \underline{\theta}^{*}_{1L\bar{\alpha}_{k}}, \underline{\theta}^{*}_{1R\bar{\alpha}_{k}}$: are the optimal vectors values of $\underline{\theta}_{1L\underline{\alpha}_{k}}, \underline{\theta}_{1R\underline{\alpha}_{k}}, \underline{\theta}_{1L\bar{\alpha}_{k}}$, and $\underline{\theta}_{1R\bar{\alpha}_{k}}$

$\gamma_{1L\bar{\alpha}_{k}x}, \gamma_{1R\bar{\alpha}_{k}x}, \gamma_{1L\underline{\alpha}_{k}x}, \gamma_{1R\underline{\alpha}_{k}x}$: are the learning rates.

Its time derivative is:

$$D^{m}V_{1}\leq e_{1}^{T}\psi+h_{\left(\gamma_{1(\alpha)L,R}\ ,\ \tilde{\theta}_{1(\alpha)L,R}\right)} \quad (37)$$

where:

$$\psi=-c_{1}e_{1}-f_{e1}+e_{2}+w_{1}-f_{\left(\zeta_{1(\alpha)L,R}^{T}\ ,\ \tilde{\theta}_{1(\alpha)L,R}\right)}$$

$$h_{\left(\gamma_{1(\alpha)L,R}\ ,\ \tilde{\theta}_{1(\alpha)L,R}\right)}=\sum_{k=1}^{N}\frac{1}{\gamma_{1L\underline{\alpha}_{k}x}}\tilde{\underline{\theta}}_{1L\underline{\alpha}_{k}}^{T}\,{}_{t_0}^{C}D_{t}^{m}\tilde{\underline{\theta}}_{1L\underline{\alpha}_{k}}+\sum_{k=1}^{N}\frac{1}{\gamma_{1R\underline{\alpha}_{k}x}}\tilde{\underline{\theta}}_{1R\underline{\alpha}_{k}}^{T}\,{}_{t_0}^{C}D_{t}^{m}\tilde{\underline{\theta}}_{1R\underline{\alpha}_{k}}+\sum_{k=1}^{N}\frac{1}{\gamma_{1L\bar{\alpha}_{k}x}}\tilde{\underline{\theta}}_{1L\bar{\alpha}_{k}}^{T}\,{}_{t_0}^{C}D_{t}^{m}\tilde{\underline{\theta}}_{1L\bar{\alpha}_{k}}+\sum_{k=1}^{N}\frac{1}{\gamma_{1R\bar{\alpha}_{k}x}}\tilde{\underline{\theta}}_{1R\bar{\alpha}_{k}}^{T}\,{}_{t_0}^{C}D_{t}^{m}\tilde{\underline{\theta}}_{1R\bar{\alpha}_{k}}$$

Based on the previous assumptions, the global convergence function is:

$$V_{2}=V_{1}+\frac{1}{2}e_{2}^{T}e_{2}+\sum_{k=1}^{N}\frac{1}{2\gamma_{2L\underline{\alpha}_{k}x}}\tilde{\underline{\theta}}_{2L\underline{\alpha}_{k}}^{T}\tilde{\underline{\theta}}_{2L\underline{\alpha}_{k}}+\sum_{k=1}^{N}\frac{1}{2\gamma_{2R\underline{\alpha}_{k}x}}\tilde{\underline{\theta}}_{2R\underline{\alpha}_{k}}^{T}\tilde{\underline{\theta}}_{2R\underline{\alpha}_{k}}+\sum_{k=1}^{N}\frac{1}{2\gamma_{2L\bar{\alpha}_{k}x}}\tilde{\underline{\theta}}_{2L\bar{\alpha}_{k}}^{T}\tilde{\underline{\theta}}_{2L\bar{\alpha}_{k}}+\sum_{k=1}^{N}\frac{1}{2\gamma_{2R\bar{\alpha}_{k}x}}\tilde{\underline{\theta}}_{2R\bar{\alpha}_{k}}^{T}\tilde{\underline{\theta}}_{2R\bar{\alpha}_{k}} \quad (38)$$

The fractional derivative is:

$$D^{m}V_{2}\leq D^{m}V_{1}+e_{2}^{T}D^{m}e_{2}+h_{\left(\gamma_{(2)L,R}\ ,\ \tilde{\theta}_{(2)L,R}\right)} \quad (39)$$

with:

$$h_{\left(\gamma_{2(\alpha)L,R}\ ,\ \tilde{\theta}_{2(\alpha)L,R}\right)}=\sum_{k=1}^{N}\frac{1}{\gamma_{2L\underline{\alpha}_{k}x}}\tilde{\underline{\theta}}_{2L\underline{\alpha}_{k}}^{T}\,{}_{t_0}^{C}D_{t}^{m}\tilde{\underline{\theta}}_{2L\underline{\alpha}_{k}}+\sum_{k=1}^{N}\frac{1}{\gamma_{2R\underline{\alpha}_{k}x}}\tilde{\underline{\theta}}_{2R\underline{\alpha}_{k}}^{T}\,{}_{t_0}^{C}D_{t}^{m}\tilde{\underline{\theta}}_{2R\underline{\alpha}_{k}}+\sum_{k=1}^{N}\frac{1}{\gamma_{2L\bar{\alpha}_{k}x}}\tilde{\underline{\theta}}_{2L\bar{\alpha}_{k}}^{T}\,{}_{t_0}^{C}D_{t}^{m}\tilde{\underline{\theta}}_{2L\bar{\alpha}_{k}}+\sum_{k=1}^{N}\frac{1}{\gamma_{2R\bar{\alpha}_{k}x}}\tilde{\underline{\theta}}_{2R\bar{\alpha}_{k}}^{T}\,{}_{t_0}^{C}D_{t}^{m}\tilde{\underline{\theta}}_{2R\bar{\alpha}_{k}}$$

Based on the following adaptation laws:

$$\begin{cases}
{}_{t_0}^{C}D_{t}^{m}\tilde{\underline{\theta}}_{1L\underline{\alpha}_{k}}=\frac{1}{2}\gamma_{1L\underline{\alpha}_{k}x}e_{1}K_{\underline{\alpha}_{k}}\xi_{L\underline{\alpha}_{k}}\\
{}_{t_0}^{C}D_{t}^{m}\tilde{\underline{\theta}}_{1R\underline{\alpha}_{k}}=\frac{1}{2}\gamma_{1R\underline{\alpha}_{k}x}e_{1}K_{\underline{\alpha}_{k}}\xi_{R\underline{\alpha}_{k}}\\
{}_{t_0}^{C}D_{t}^{m}\tilde{\underline{\theta}}_{2L\underline{\alpha}_{k}}=\frac{1}{2}\gamma_{2L\underline{\alpha}_{k}x}e_{2}K_{\underline{\alpha}_{k}}\xi_{L\underline{\alpha}_{k}}\\
{}_{t_0}^{C}D_{t}^{m}\tilde{\underline{\theta}}_{2R\underline{\alpha}_{k}}=\frac{1}{2}\gamma_{2R\underline{\alpha}_{k}x}e_{2}K_{\underline{\alpha}_{k}}\xi_{R\underline{\alpha}_{k}}\\
{}_{t_0}^{C}D_{t}^{m}\tilde{\underline{\theta}}_{1L\bar{\alpha}_{k}}=\frac{1}{2}\gamma_{1L\bar{\alpha}_{k}x}e_{1}K_{\bar{\alpha}_{k}}\xi_{L\bar{\alpha}_{k}}\\
{}_{t_0}^{C}D_{t}^{m}\tilde{\underline{\theta}}_{1R\bar{\alpha}_{k}}=\frac{1}{2}\gamma_{1R\bar{\alpha}_{k}x}e_{1}K_{\bar{\alpha}_{k}}\xi_{R\bar{\alpha}_{k}}\\
{}_{t_0}^{C}D_{t}^{m}\tilde{\underline{\theta}}_{2L\bar{\alpha}_{k}}=\frac{1}{2}\gamma_{2L\bar{\alpha}_{k}x}e_{2}K_{\bar{\alpha}_{k}}\xi_{L\bar{\alpha}_{k}}\\
{}_{t_0}^{C}D_{t}^{m}\tilde{\underline{\theta}}_{2R\bar{\alpha}_{k}}=\frac{1}{2}\gamma_{2R\bar{\alpha}_{k}x}e_{2}K_{\bar{\alpha}_{k}}\xi_{R\bar{\alpha}_{k}}
\end{cases} \quad (40)$$

Remark 2: The learning rates ($\gamma_{1L\underline{\alpha}_{k}x}$, $\gamma_{1R\underline{\alpha}_{k}x}$,$\gamma_{1L\bar{\alpha}_{k}x}$, $\gamma_{1R\bar{\alpha}_{k}x}$,$\gamma_{2L\underline{\alpha}_{k}x}$, $\gamma_{2R\underline{\alpha}_{k}x}$,$\gamma_{2L\bar{\alpha}_{k}x}$, and $\gamma_{2R\bar{\alpha}_{k}x}$) of the adaptation laws can be tuned by trial and error or obtained by using one of optimization algorithms presented in the literature.

Finally, the global stability of the closed loop system is proved by the following expression:

$$D^{m}V_{2}<-c_{1}e_{1}^{T}e_{1}-c_{2}e_{2}^{T}e_{2} \quad (41)$$

with c_1 and c_2 are strictly positive constants.

TABLE 2. DFIG parameters.

Parameters	Values	Units
Stator resistance (R_s)	2.25	[Ω]
Rotor resistance (R_r)	0.7	[Ω]
Stator inductance (L_s)	0.1232	[H]
Rotor inductance (L_r)	0.1122	[H]
Nr. of pole pairs (P)	2	-

TABLE 3. Nomenclature.

Case	Approach
Case 01	Classical Backstepping Control
Case 02	FT-1 Backstepping Control
Case 03	FT-2 Backstepping Control
Case 04	FGT-2 Backstepping Control
Case 05	proposed approach

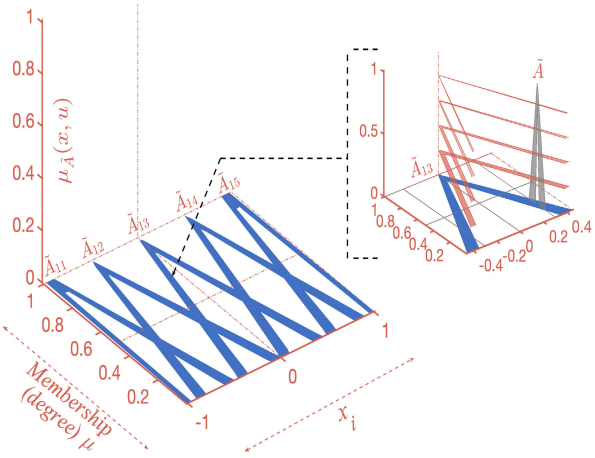

FIGURE 6. Used membership functions.

IV. SIMULATIONS AND RESULTS

In this section, the proposed approach's performance is analyzed in two steps: In the first step, we compare the control system response of our approach with those of the other backstopping based approaches under parameter variations and external disturbances. The second step, a comparative study is done with other approaches published in the literature. Noted that simulations have been carried out using MATLAB with a 1.5 kW DFIG whose parameters are presented in Table 2. For the fuzzy logic part, five fuzzy sets (shown in Fig. 6), were used for each input of the fuzzy system. Triangular fuzzy membership functions were chosen because of their simple formulas and reduced computation time. In the following, we use the nomenclature given by Table 3.

Remark 3: In this paper, the particle swarm optimization (PSO) computational method [34] (with the specifications presented in Table 4) is used to tune the parameters of the proposed nonlinear controller. The convergence of the PSO optimization algorithm in terms of the objective function

TABLE 4. PSO parameters.

parameters	Values
Number of particles (n)	50
Maximum number of iteration (Nm)	100
Inertia factor (w)	0.7
Positive constant used to update the particle velocity (C)	2

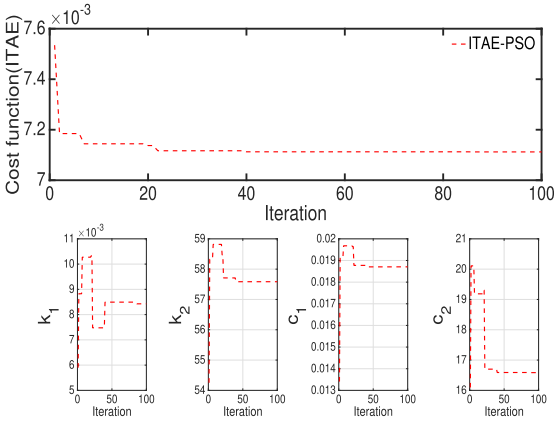

FIGURE 7. Objective function convergence/parameters tuning.

(where the Integral Time Absolute Error $ITAE = \int_0^t (t|e(t)|)dt$ is used to evaluate system responses) with the number of iterations is shown in Fig.7.

A. DFIG UNDER EXTERNAL DISTURBANCES

Simulation results for DFIG in the presence of external disturbances using the approaches cited in Table 3 are given by Figs 8 to 12. The obtained results show the superiority of the proposed controller, which benefits from new interval type 3 fuzzy logic compared to the other backstepping approaches (case 01 to 04). These results show the following improvements:

- Response time of both flux and velocity tracking is enhanced (Figs 8 and 9)
- Both oscillation and transition phase of power responses are reduced (Fig.10)
- Both oscillation and transition phase of the voltage/current signals applied to the rotor are also reduced (Fig.11)

B. DFIG UNDER PARAMETRIC VARIATIONS

The second test considered is related to the effect of temporary variations of the mutual inductance (L_m) on the system performances using the approaches of Table 3. These variations are introduced respectively at $t = 6.25\ sec$ (from 0 to 40%) then at $t = 18.75\ sec$ (from 0 to 45%). It should be noted that this simulation test does not involve any external disturbances.

Simulation results (tracking errors Figs. 13 and 14, transition phases of the control signals Fig. 15, and output signal

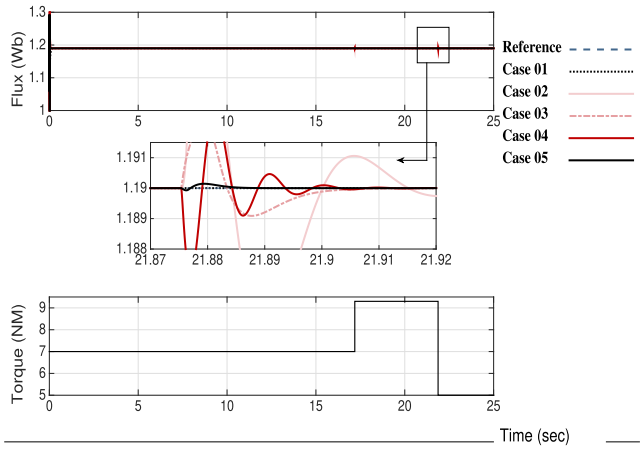

FIGURE 8. Generator torque and flux.

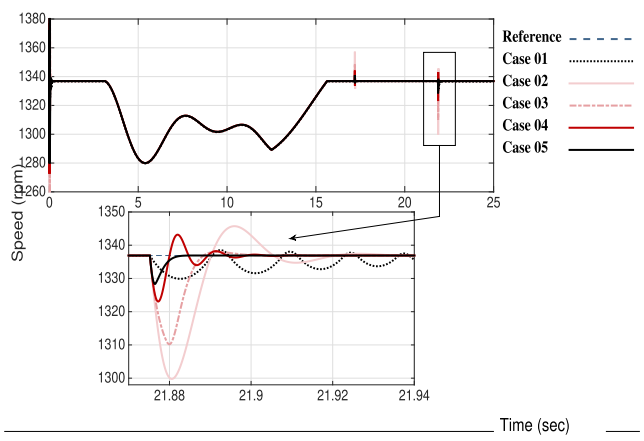

FIGURE 9. Mechanical speed.

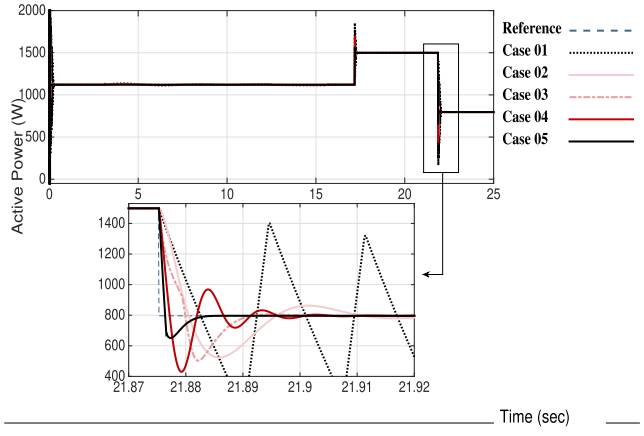

FIGURE 10. Stator power.

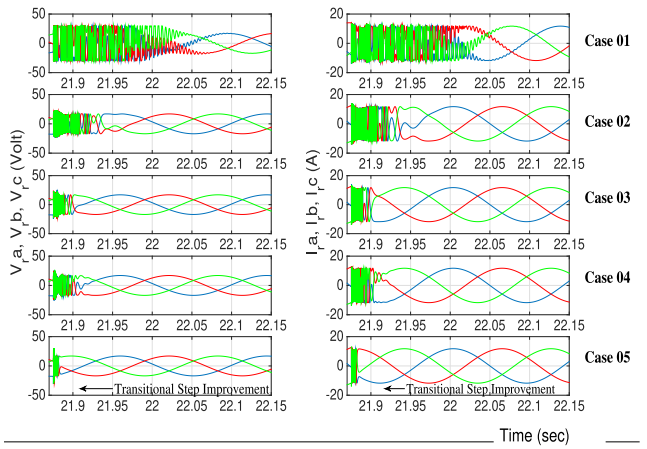

FIGURE 11. Rotor voltages and currents.

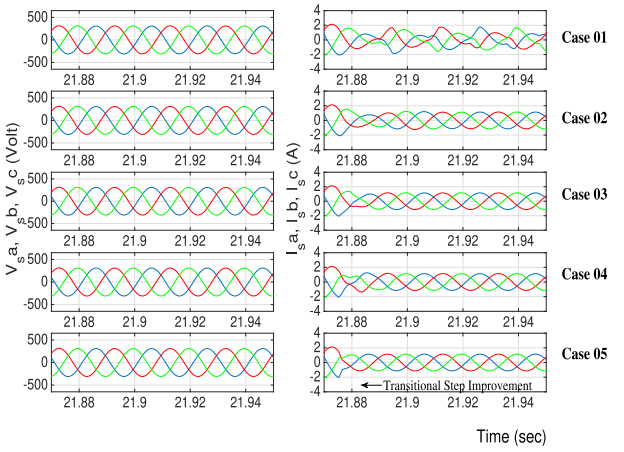

FIGURE 12. Stator voltages and currents.

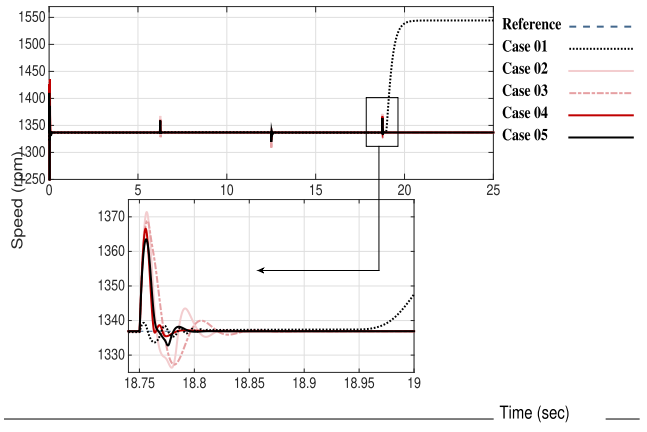

FIGURE 13. Mechanical speed during L_m varying.

waveforms Fig. 16) reveal the effectiveness and superiority of the proposed approach where FT-3 systems provide a better approximation capability compared to the other studied fuzzy systems. Indeed, during the $_Lm$ variation step, the proposed method (case 05) demonstrates a minimum fluctuation of the DFIG signal response and leads to a minimum level of voltage transitory phases. These observations are also confirmed by the values of the error evaluation criteria (given in Table 5), which highlight a significant improvement in the average error; around 88% compared to the FT1 fuzzy approach, 72%

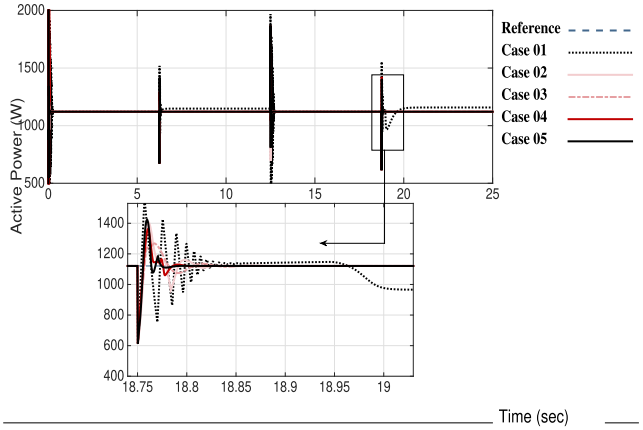

FIGURE 14. Stator power during L_m varying.

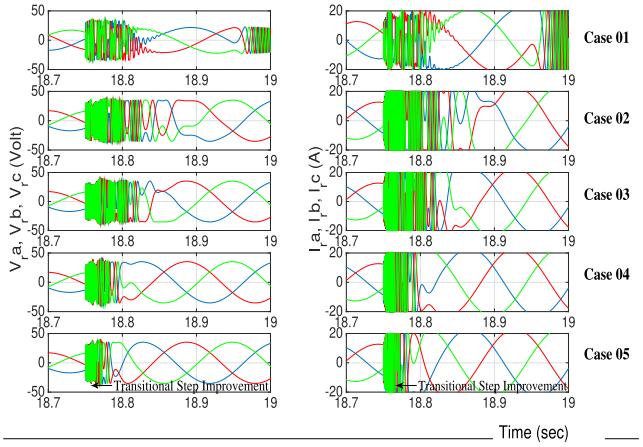

FIGURE 15. Rotor voltages and currents during L_m varying.

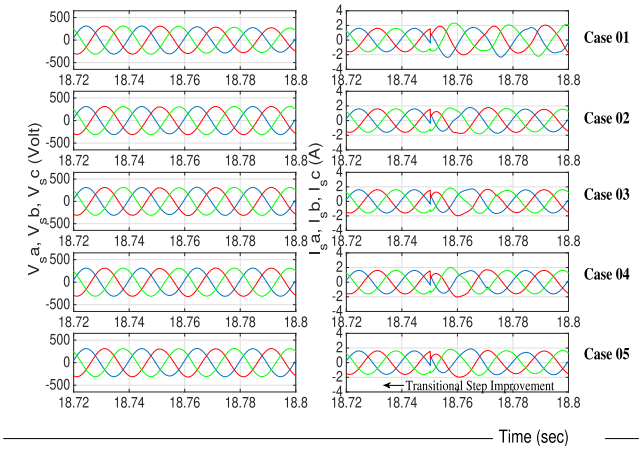

FIGURE 16. Stator voltages and currents during L_m varying.

TABLE 5. ISE, ITAE Performance indices values under L_m varying.

ISE

Approaches	Ω_r	φ	Average
Backstepping	2.2491	2.3951e+05	1.1976e+05
FT1-FLS Backstepping	0.0010295	509.94	254.97
FIT2-FLS Backstepping	0.00033353	216.05	108.02
FGT2-FLS Backstepping	0.00059903	141.56	70.782
FIT3-FLS Backstepping	0.00017439	58.027	29.013

ITAE

Approaches	Ω_r	φ	Average
Backstepping	85.344	26283	13184
FT1-FLS Backstepping	0.016748	18.797	9.407
FIT2-FLS Backstepping	0.023005	15.734	7.8784
FGT2-FLS Backstepping	0.016233	9.0549	4.5356
FIT3-FLS Backstepping	0.013762	7.8404	3.9271

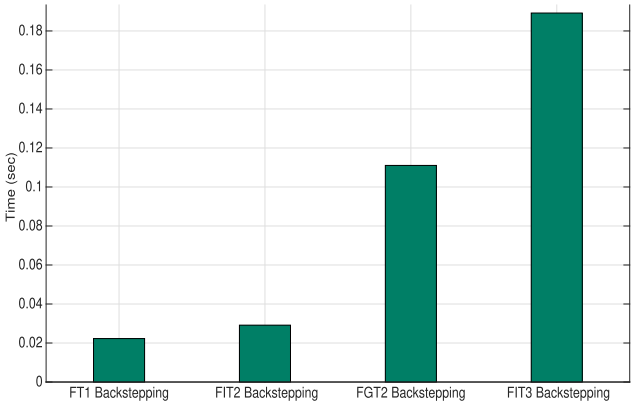

FIGURE 17. Computation times.

TABLE 6. Comparison with other approaches.

Publication paper	Technical methods	Response time(s)	Error (%)
[35]	Fuzzy field oriented control	1	-
[36]	Double Integral SMC	0.003	0.006
[37]	Sliding-Backstepping mode control	0.03	0.09
[38]	PI	0.030	1.25
	RST	0.028	0.06
[39]	Observer Sliding Mode Control	0.015	0.15
[40]	Hybrid SMC Backstepping	0.069	0.2
Proposed technique	FIT3 Backstepping	0.005	0.0013

compared to the FIT2-FLS and finally 59% compared to the FGT2 fuzzy technique.

The computational cost is related to the complexity and design parameters of the control methods. However, it should be noted that the proposed approach (FIT3-FLS backstepping) remains bearable considering the advantages of the control methods and the nature of the applications (Fig. 17).

C. COMPARISON WITH OTHER APPROACHES

Finally, to demonstrate the efficiency and advantages of the proposed method, simulation results are compared with other

works published in the literature. The comparison results, which are reported in Table 6, demonstrate the superiority of the proposed approach in terms of response time and accuracy for output power. Nevertheless, it should be noted that it is difficult to find in the literature works proposing control techniques carried out under the same conditions. Therefore, the comparison focuses only on some aspects of DFIG control.

V. CONCLUSION

In this article, a novel fractional backstepping control method based on interval type 3 adaptive fuzzy logic systems (IT3-FLSs) is designed for a doubly fed induction generator. The resulting control laws aim to improve the tracking performance and increase the system's robustness especially in the presence of external disturbances and variations in generator parameters. A fractional Lyapunov analysis is used to prove the stability of the system. Simulations demonstrate the effectiveness of the proposed control approach compared to other adaptive fuzzy backstepping methods (GT2 FLS, IT2 FLS, and T1 FLS). In the near future, this method constitutes a promising control approach to be implemented.

REFERENCES

[1] P. K. Gayen, D. Chatterjee, and S. K. Goswami, "A low-voltage ride-through capability enhancement scheme of doubly fed induction generator based wind plant considering grid faults," *J. Renew. Sustain. Energy*, vol. 8, no. 2, Mar. 2016, Art. no. 025301.

[2] P. Cheng, H. Nian, C. Wu, and Z. Q. Zhu, "Direct stator current vector control strategy of DFIG without phase-locked loop during network unbalance," *IEEE Trans. Power Electron.*, vol. 32, no. 1, pp. 284–297, Jan. 2017.

[3] B. Desalegn, D. Gebeyehu, and B. Tamrat, "Evaluating the performances of PI controller (2DOF) under linear and nonlinear operations of DFIG-based WECS: A simulation study," *Heliyon*, vol. 8, no. 12, Dec. 2022, Art. no. e11912.

[4] T. Cheng, J. Wu, H. Wang, and H. Zheng, "Dynamic optimization of rotor-side PI controller parameters for doubly-fed wind turbines based on improved recurrent neural networks under wind speed fluctuations," *IEEE Access*, vol. 11, pp. 102713–102726, 2023.

[5] M. S. Arifin, M. N. Uddin, and W. Wang, "Neuro-fuzzy adaptive direct torque and flux control of a grid-connected DFIG-WECS with improved dynamic performance," *IEEE Trans. Ind. Appl.*, vol. 59, no. 6, pp. 7692–7700, Nov. 2023.

[6] D. Jiang, W. Yu, J. Wang, G. Zhong, and Z. Zhou, "Dynamic analysis of DFIG fault detection and its suppression using sliding mode control," *IEEE J. Emerg. Sel. Topics Power Electron.*, vol. 11, no. 1, pp. 643–656, Feb. 2023.

[7] N. Dahri and M. Ouassaid, "Tracking performance and power quality enhancement of DFIG based wind turbine using robust integral terminal sliding mode control," *e-Prime Adv. Electr. Eng., Electron. Energy*, vol. 10, Dec. 2024, Art. no. 100784.

[8] S. Puchalapalli and B. Singh, "A single input variable FLC for DFIG-based WPGS in standalone mode," *IEEE Trans. Sustain. Energy*, vol. 11, no. 2, pp. 595–607, Apr. 2020.

[9] A. Chakraborty and T. Maity, "An adaptive fuzzy logic control technique for LVRT enhancement of a grid-integrated DFIG-based wind energy conversion system," *ISA Trans.*, vol. 138, pp. 720–734, Jul. 2023.

[10] J. Liu, Y. Gao, S. Geng, and L. Wu, "Nonlinear control of variable speed wind turbines via fuzzy techniques," *IEEE Access*, vol. 5, pp. 27–34, 2017.

[11] S. K. Raju and G. N. Pillai, "Design and implementation of type-2 fuzzy logic controller for DFIG-based wind energy systems in distribution networks," *IEEE Trans. Sustain. Energy*, vol. 7, no. 1, pp. 345–353, Jan. 2016.

[12] H. M. Moghadam, M. Gheisarnejad, Z. Esfahani, and M.-H. Khooban, "A novel supervised control strategy for interconnected DFIG-based wind turbine systems: MiL validations," *IEEE Trans. Emerg. Topics Comput. Intell.*, vol. 5, no. 6, pp. 962–971, Dec. 2021.

[13] B. Bossoufi, M. Karim, M. Taoussi, H. A. Aroussi, M. Bouderbala, O. Deblecker, S. Motahhir, A. Nayyar, and M. A. Alzain, "Rooted tree optimization for the backstepping power control of a doubly fed induction generator wind turbine: DSPACE implementation," *IEEE Access*, vol. 9, pp. 26512–26522, 2021.

[14] M. Morawiec, K. Blecharz, and A. Lewicki, "Sensorless rotor position estimation of doubly fed induction generator based on backstepping technique," *IEEE Trans. Ind. Electron.*, vol. 67, no. 7, pp. 5889–5899, Jul. 2020.

[15] A. Loulijat, M. Makhad, A. Hilali, H. Chojaa, M. El Marghichi, M. Hatatah, and T. A. H. Alghamdi, "Enhancing fault ride-through capacity of DFIG-based WPs by adaptive backstepping command using parametric estimation in non-linear forward power controller design," *IEEE Access*, vol. 12, pp. 58675–58689, 2024.

[16] A. Tarek, H. Abdelaziz, E. Najib, and B. Farid, "An adaptive backstepping controller of doubly-fed induction generators," in *Proc. 3rd Int. Conf. Control, Eng. Inf. Technol. (CEIT)*, Tlemcen, Algeria, May 2015, pp. 1–6.

[17] J. M. Mendel, *Uncertain Rule-Based Fuzzy Logic Systems*. Upper Saddle River, NJ, USA: Prentice-Hall, 2001.

[18] J. M. Mendel, "Uncertain rule-based fuzzy systems," in *Introduction and New Directions*, vol. 684. Cham, Switzerland: Springer, 2017.

[19] S. Issaouni, A. Boulkroune, and H. Chekireb, "Adaptive fuzzy backstepping controller of induction machine," in *Proc. 4th Int. Conf. Electr. Eng. (ICEE)*, Boumerdes, Algeria, Dec. 2015, pp. 1–6.

[20] A. Sakouchi, A. Djahbar, E. Bounadja, H. Benbouhenni, A. Iqbal, A. Moualdia, and A. Kechida, "Enhanced control of grid-connected multi-machine wind power generation systems using fuzzy backstepping approaches," *Energy Rep.*, vol. 12, pp. 4208–4231, Dec. 2024.

[21] N. Ezziani, A. Hussain, N. Essounbouli, and A. Hamzaoui, "Backstepping adaptive type-2 fuzzy controller for induction machine," in *Proc. IEEE Int. Symp. Ind. Electron.*, Jun. 2008, pp. 443–448.

[22] J. Z. Shi, "A fractional order general type-2 fuzzy PID controller design algorithm," *IEEE Access*, vol. 8, pp. 52151–52172, 2020.

[23] A. Kumar, R. Raj, and A. Mohammadzadeh, "Recent advancements in type-3 fuzzy logic systems: A comprehensive review," *IEEE Trans. Emerg. Topics Comput. Intell.*, pp. 1–14, Jul. 2024.

[24] G. M. Mendez, I. Lopez-Juarez, P. N. Montes-Dorantes, and M. A. Garcia, "A new method for the design of interval type-3 fuzzy logic systems with uncertain type-2 non-singleton inputs (IT3 NSFLS-2): A case study in a hot strip mill," *IEEE Access*, vol. 11, pp. 44065–44081, 2023.

[25] A. Mohammadzadeh, M. H. Sabzalian, and W. Zhang, "An interval Type-3 fuzzy system and a new online fractional-order learning algorithm: Theory and practice," *IEEE Trans. Fuzzy Syst.*, vol. 28, no. 9, pp. 1940–1950, Sep. 2020.

[26] S. Adigintla and M. V. Aware, "Robust fractional order speed controllers for induction motor under parameter variations and low speed operating regions," *IEEE Trans. Circuits Syst. II, Exp. Briefs*, vol. 70, no. 3, pp. 1119–1123, Mar. 2023.

[27] H. Benbouhenni, M. I. Mosaad, I. Colak, N. Bizon, H. Gasmi, M. Aljohani, and E. Abdelkarim, "Fractional-order synergetic control of the asynchronous generator-based variable-speed multi-rotor wind power systems," *IEEE Access*, vol. 11, pp. 133490–133508, 2023.

[28] S. Luo, Y. Song, F. L. Lewis, R. Garrappa, and S. Li, "Dynamic analysis and fuzzy fixed-time optimal synchronization control of unidirectionally coupled FO permanent magnet synchronous generator system," *IEEE Trans. Fuzzy Syst.*, vol. 31, no. 5, pp. 1742–1755, May 2023.

[29] Y. Zhang, Y. Lyu, S. Hou, S. Xue, and H. Liu, "Modeling and chaos dynamics analysis of doubly-fed induction generator based on incommensurate fractional-order," *IEEE Trans. Energy Convers.*, vol. 40, no. 2, pp. 911–927, Jun. 2025.

[30] A. Dani, M. Benlamlih, Z. Mekrini, M. El Mrabet, and M. Boulaala, "Wind energy conversion technologies and control strategies: A review," *Int. J. Renew. Energy Res.*, vol. 14, no. 1, pp. 140–154, 2024.

[31] P. Melin and O. Castillo, "An interval type-3 fuzzy–fractal approach for plant monitoring," *Axioms*, vol. 12, no. 8, p. 741, Jul. 2023.

[32] I. Petráš, *Fractional-Order Nonlinear Systems: Modeling, Analysis and Simulation*. Cham, Switzerland: Springer, 2011.

[33] N. Aguila-Camacho, M. A. Duarte-Mermoud, and J. A. Gallegos, "Lyapunov functions for fractional order systems," *Commun. Nonlinear Sci. Numer. Simul.*, vol. 19, no. 9, pp. 2951–2957, Sep. 2014.
[34] A. Baraean, W. M. Hamanah, A. Bawazir, M. M. Quama, S. E. Ferik, S. Baraean, and M. A. Abido, "Optimal nonlinear backstepping controller design of a quadrotor-slung load system using particle swarm optimization," *Alexandria Eng. J.*, vol. 68, pp. 551–560, Apr. 2023.
[35] C.-M. Hong, C.-H. Chen, and C.-S. Tu, "Maximum power point tracking-based control algorithm for PMSG wind generation system without mechanical sensors," *Energy Convers. Manage.*, vol. 69, pp. 58–67, May 2013.
[36] J. Hostettler and X. Wang, "Sliding mode control of a permanent magnet synchronous generator for variable speed wind energy conversion systems," *Syst. Sci. Control Eng.*, vol. 3, no. 1, pp. 453–459, Jan. 2015.
[37] F. Echiheb, Y. Ihedrane, B. Bossoufi, M. Bouderbala, S. Motahhir, M. Masud, S. Aljahdali, and M. ElGhamrasni, "Robust sliding-backstepping mode control of a wind system based on the DFIG generator," *Sci. Rep.*, vol. 12, no. 1, Jul. 2022, Art. no. 11782.
[38] B. Bossoufi, M. Karim, A. Lagrioui, and M. Taoussi, "FPGA-based implementation sliding mode control and nonlinear adaptive backstepping control of a permanent magnet synchronous machine drive," *Wseas Trans. Syst. Control*, vol. 9, pp. 86–100, Feb. 2014.
[39] H. E. Alami, B. Bossoufi, S. Motahhir, E. H. Alkhammash, M. Masud, M. Karim, M. Taoussi, M. Bouderbala, M. Lamnadi, and M. El Mahfoud, "FPGA in the loop implementation for observer sliding mode control of DFIG-generators for wind turbines," *Electronics*, vol. 11, no. 1, p. 116, Dec. 2021.
[40] F. Echiheb, I. Elkafazi, B. Bossoufi, B. El Bhiri, M. M. Almalki, and T. A. H. Alghamdi, "Nonlinear robust sliding mode–backstepping hybrid control for WECS-theoretical design and experimental evaluation," *Heliyon*, vol. 10, no. 11, Jun. 2024, Art. no. e31767.

TAREK AOUNALLAH received the Ph.D. degree in electronic instrumentation from the University of Science and Technology Houari Boumediene, Algiers, Algeria, in 2020. He is currently a Teacher with the University of Reims Champagne-Ardenne. His research interests include nonlinear control approaches (backstepping, fuzzy logic systems, sliding mode, and fractional order calculus) applied to renewable energies, automated glycemia control in type 1 diabetic patients and robotics.

NAWAL FERHAT received the Magister degree in electronic instrumentation from the University of Science and Technology Houari Boumediene, Algiers, Algeria, in 2013, where she is currently pursuing the Ph.D. degree. Her research interests include nonlinear control (adaptive fuzzy control, high order sliding mode control, backstepping control method, and fractional order systems) applied to renewable energies, automated control of blood glucose in diabetes mellitus type 1 patients and robotics.

NAJIB ESSOUNBOULI received the Ph.D. and Habilitation degrees from Reims Champagne Ardenne University, in 2004 and 2009, respectively, all in control engineering. Since September 2010, he has been an Assistant Professor with the University of Reims Champagne-Ardenne, IUT of Troyes, where he has been a Professor, since September 2010. He was the Head of Mechanical Engineering Department, University of Reims Champagne-Ardenne, IUT of Troyes, from 2014 to 2020. Actually, he is the Head of the TICA Team (CReSTIC Laboratory) and he works on nonlinear control (fuzzy logic, high order sliding modes, and fractional order systems) applied to renewable energy and robotics.

ABDELAZIZ HAMZAOUI received the degree in electrical engineering from the Polytechnic School of Algiers, Algeria, in 1982, and the D.E.A. and Ph.D. degrees from the University of Reims Champagne-Ardenne, Troyes, France, both in electrical engineering, in 1989 and 1992, respectively. He is a currently a Professor with the Technology Institute of Troyes, University of Reims Champagne-Ardenne, where he was the Director. His research interests include intelligent control, fuzzy control, and robust adaptive control.